Anomalous Aharonov-Bohm Conductance Oscillations from Topological Insulator Surface States

Yi Zhang[1,2] and Ashvin Vishwanath[1,2]

[1]*Department of Physics, University of California at Berkeley, Berkeley, California 94720, USA*
[2]*Materials Sciences Division, Lawrence Berkeley National Laboratory, Berkeley, California 94720, USA*

(Received 20 May 2010; revised manuscript received 7 July 2010; published 11 November 2010)

We study Aharonov-Bohm (AB) conductance oscillations arising from the surface states of a topological insulator nanowire, when a magnetic field is applied along its length. With *strong* surface disorder, these oscillations are predicted to have a component with anomalous period $\Phi_0 = hc/e$, twice the conventional period. The conductance maxima are achieved at odd multiples of $\frac{1}{2}\Phi_0$, implying that a π AB phase for electrons strengthens the metallic nature of surface states. This effect is special to topological insulators, and serves as a defining transport property. A key ingredient, the surface curvature induced Berry phase, is emphasized here. We discuss similarities and differences from recent experiments on Bi_2Se_3 nanoribbons, and optimal conditions for observing this effect.

DOI: 10.1103/PhysRevLett.105.206601 PACS numbers: 72.20.My, 73.20.Fz

There has been much recent interest in topological insulators (TIs), three-dimensional insulators with metallic surface states protected by time reversal ($\mathcal{T}$) invariance (see [1] for reviews). Surface sensitive experiments such as angle-resolved photoemission spectroscopy (ARPES) and STM [1], have confirmed the existence of this exotic surface metal, which, in its simplest form, takes a single Dirac dispersion. However, so far there have been no transport experiments verifying the topological nature of the surface states. Besides the fact that bulk impurity bands may contribute significantly to conductivity, the key transport property is the absence of localization when $\mathcal{T}$ invariance is present. This has been hard to convert into a clear-cut experiment. Here we discuss a topological feature of TI surface states that leads to a transport signature, which we believe is experimentally accessible. The Aharonov-Bohm effect will play a central role. Also, the Berry phase for electrons propagating on the curved surface of a topological insulator will be important. We model this as a Dirac theory in curved space, drawing on ideas developed to study fermions in curved space-time [2].

Consider a wire of topological insulator, with magnetic flux applied along its length. The surface states see flux and can be considered a collection of one-dimensional (1D) modes, that come in pairs moving up and down the wire. Throughout we assume low temperatures so the thermal dephasing length exceeds the sample dimensions. Time reversal symmetry is present at zero flux, and also, approximately for the surface states, when the surface encloses an integer multiple of $\frac{1}{2}\Phi_0$ ($= hc/2e$) flux quanta. However, there is an important difference between even and odd multiples of $\frac{1}{2}\Phi_0$ flux. Odd multiples of $\frac{1}{2}\Phi_0$ flux lead to a π Aharonov-Bohm phase for surface electrons, resulting in an *odd* number of pairs of modes [3,4]. This can be seen from a simple model of TI surface states: a single Dirac cone. These Dirac excitations are sensitive to surface geometry, since the physical spin is locked to surface orientation. Hence they behave like Dirac particles in a curved two-dimensional space. There is no analog of this for graphene rolled up into nanotubes, since there the Dirac matrices act on an internal pseudospin space. Hence surface curvature introduces an additional Berry's phase of π on circling the cylindrical surface of a topological insulator, as shown in [3], and below. This 1D state is topologically protected and cannot be localized with $\mathcal{T}$ symmetry [5]. In contrast, even multiples of $\frac{1}{2}\Phi_0$ flux lead to an even number of modes which are not protected. In this Letter we build on this observation a sharp transport signature in the presence of strong disorder. For a wire of fixed length with sufficiently strong disorder, even flux leads to a fully localized state while odd flux leads to a metallic state whose conductance ideally approaches e^2/h. We show this can survive despite time reversal symmetry breaking from the magnetic field, which is present at all fluxes.

Note, this oscillatory dependence has a flux $\Phi_0 = hc/e$ period, in contrast to Aharonov-Altshuler-Spivak (AAS) oscillations which have period $\frac{1}{2}\Phi_0 = hc/2e$. There has been much discussion on the question of Φ_0 vs $\frac{1}{2}\Phi_0$ oscillations, in mesoscopic rings [6,7] and cylinders [8,9]. For rings, both periods are observed, the first period is attributed to AB interference of single electrons, and the second to AAS oscillation. The period doubling of the latter arises from weak localization (or antilocalization) effects which involve pairs of time reversed paths. However, in metallic cylinders, only the $\frac{1}{2}\Phi_0$ period has been experimentally reported [8]. The Φ_0 period has been theoretically predicted [7,9], but occurs with random phase, i.e., can peak at either even or odd multiples of $\frac{1}{2}\Phi_0$. Therefore an ensemble average tends to wash out this effect, which, according to Refs. [6,7], is why the $\frac{1}{2}\Phi_0$ effect is more commonly observed.

In contrast, the period $\Phi_0 = hc/e$ oscillation described here is unique in having maxima *always* at odd-integer multiples of $\frac{1}{2}\Phi_0$, and only occurs in strong TIs.

A recent experiment on topological insulator Bi_2Se_3 nanowires has indeed reported such an anomalous hc/e flux period [10]. However, there is a crucial difference from the effect described above—the conductivity is found to be minimum at the locations of the predicted maxima. Hence Ref. [10] must be observing different physics, perhaps analogous to the Φ_0 oscillation of [6]. We point out one possible mechanism for this at weak disorder. The regime described in this Letter is accessed by going to strong disorder on the surface. The current experiments demonstrate coherent quantum transport from surface states, which is a hopeful sign for accessing the physics of this Letter in future experiments with strong disorder.

We first describe the physical ingredients that give rise to this anomalous AB effect, in clean systems. Subsequently, we report the result of numerical experiments on disordered cylinders of topological insulators, realized in a three-dimensional lattice model.

Analytic surface Dirac theory.—Consider generalizing the Dirac Hamiltonian for a flat surface perpendicular to the z direction $H = -iv_F\hbar(p_x\sigma_x + p_y\sigma_y)$ to the case when the surface is curved. We utilize the fact that the surface is embedded in three-dimensional space, so $\mathbf{r}(x^1, x^2)$ is the three-vector defining the surface location, as the surface coordinates x^i $(i = 1, 2)$ are varied. Then, $\mathbf{e}_i = \partial\mathbf{r}/\partial x^i$ are tangent vectors. Define conjugate tangent vectors $\mathbf{e}^i$, via $\mathbf{e}^i \cdot \mathbf{e}_j = \delta_{ij}$, the Kronecker delta function. Naively, one might guess that the Dirac equation on this curved surface is just $H_1 = -iv_F\hbar(\alpha^1\partial_1 + \alpha^2\partial_2)$, where $\partial_i = \partial_{x^i}$ and $\alpha^i = \mathbf{e}^i \cdot \sigma$ are the Pauli matrices along the tangent vectors. However, the actual form for a Dirac equation in curved space is $H_D = -i\hbar v_F(\alpha^1 D_1 + \alpha^2 D_2)$, where D_i is the covariant derivative along a pair of coordinates x^i, defined as $D_i = \partial_i + \Gamma_i$, where Γ_i is the spin connection which, in our case, is given in terms of [11] $\beta = \mathbf{e}^3 \cdot \sigma$ (the Pauli matrix along the surface normal $\mathbf{e}^3 = \mathbf{e}^1 \times \mathbf{e}^2/|\mathbf{e}^1 \times \mathbf{e}^2|$) as $\Gamma_i = -\frac{1}{2}\beta\partial_i\beta$

Now, let us specialize to a cylindrical surface such that $x^1 = z$ along the cylinder axis and $x^2 = R\theta$, where R is the radius and θ is the angle around the cylinder. Using $\beta = -(\cos\theta\sigma_x + \sin\theta\sigma_y)$ one can derive Γ_i from the relation above to obtain $H_D = -i\hbar v_F(\sigma_z\partial_z + \sigma_\theta\partial_\theta/R + \beta/2R)$, where $\sigma_\theta = (\cos\theta\sigma_y - \sin\theta\sigma_x)$. The unitary transformation $U = e^{i\sigma_z\theta/2}$ transforms this into the canonical form $H_D' = -i\hbar v_F(\sigma_z\partial_z + \sigma_y\partial_\theta/R)$. However, since the unitary transformation changes sign $\theta \to \theta + 2\pi$, the wave functions for the new Hamiltonian satisfy *antiperiodic* boundary conditions on circling the cylinder. Therefore, only angular momenta $\hbar(m + 1/2)$ are allowed, where m is integer. Hence, the zero angular momentum is absent, and there are an even number of one-dimensional modes pairs. Now threading an additional π flux, the periodic boundary conditions are restored, and the parity of the mode pairs is reversed; see [11] for a more general argument. Although the cylinder has vanishing Gaussian curvature, a nonzero spin connection leads to the Berry's phase of π. This topological property is also ultimately responsible for metallic dislocation lines [3,12].

Microscopic model.—We now demonstrate this effect for a lattice model of a strong topological insulator (which is more general than the Dirac approximation). We use the model of Fu-Kane-Mele [13] on the diamond lattice. Parameters are chosen to give a strong topological insulator [11] with bulk gap $\Delta = 2t$. A long cuboid with cross section $L \times L$ is taken along the weak index direction of this model, and surface states are labeled by momenta k_z along the long axis. A uniform magnetic flux Φ is introduced uniformly through the cross section, denoted in units of the flux quantum: $\varphi = 2\pi\Phi/\Phi_0$. The surface spectrum is shown in Fig. 1. All modes are doubly degenerate except the linearly dispersing mode in 1(d). Thus, even for small sizes $L = 10$, the even-odd mode effect and the gap closing at flux $\varphi = \pi$ is apparent. While the breaking of time reversal symmetry at this flux implies there is always a gap, this is seen to be very small, and the curves appear 2π periodic, so time reversal is approximately a good symmetry at these flux values. Thus, even in the clean limit, metallic behavior appears at odd multiples of π flux, for a carefully tuned chemical potential near the node. However,

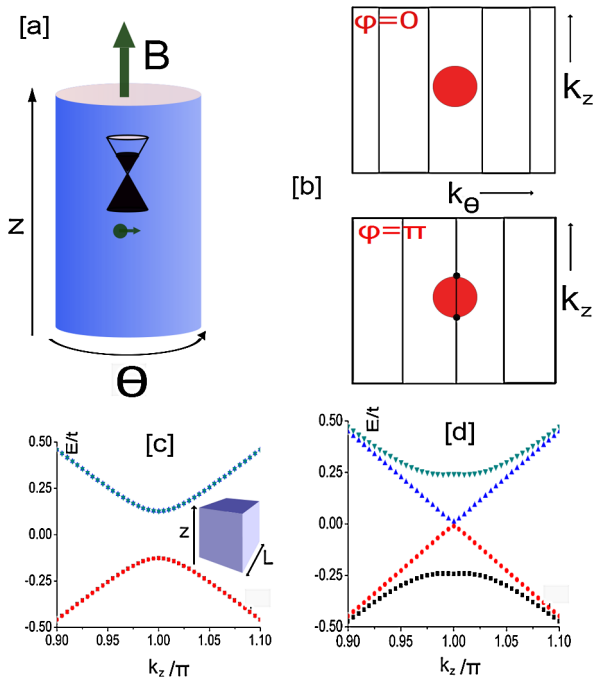

FIG. 1 (color online). (a) proposed geometry, with (weak) magnetic field applied along z with flux $\varphi = 2\pi\Phi/\Phi_0$. (b) Quantization of transverse momenta k_θ for a cylinder, as a function of applied flux. The Fermi sea is shaded. For $\varphi = 0$, an even number of 1D mode pairs occurs; but with $\varphi = \pi$ flux, an odd number of pairs is expected. Numerical demonstration in a microscopic model: spectrum of a cuboid of clean topological insulator, with cross section 10×10 unit cells (geometry shown in inset), as a function of momentum k_z along its length. (c) Spectrum for $\varphi = 0$, each band shown is doubly degenerate. (d) For flux $\varphi = \pi$, all modes except the linear one are doubly degenerate; hence an odd number of 1D mode pairs is present.

on raising the Fermi energy, the flux strength with the larger number of modes oscillates between flux zero and π, the former is reminiscent of the experimentally observed AB oscillations [10]. A robust response, however, is exposed by the presence of strong disorder, which we discuss next.

Disordered system.—We now consider adding disorder *only* on the surfaces of the model above, via a random on-site potential $V_i n_i$, ($\mathcal{T}$ invariant disorder), where n_i is the charge density on site, and V_i a random variable picked from a box distribution $[-W, W]$. We calculate the Greens function for a system composed of N layers in the z direction, and transverse size $L \times L$, at energy E: $G_N(r, r'; E)$. The position and spin coordinates are lumped into r. The transport properties of the surface states are characterized by extracting the localization length of the system in the quasi-one-dimensional limit. The technical simplification for localization length λ is that one only needs the Greens function between the first and last layers of the system, as the system length is increased. Denote by the matrix $\mathbf{G}^{(N+1)}_{1,N+1}$, the Greens function between the first and last layers of a system with $N+1$ layers, where the matrix indices refer to sites in the layer, and the energy label is suppressed. The localization length: $\lambda^{-1} = \lim_{N\to\infty} \frac{-2}{N} \log(|\mathbf{G}^{(N+1)}_{1,N+1}|^2)$, which is self-averaging, is extracted by a linear fit [an example is shown in Fig. 2(a) inset] to the logarithm of the Greens function. The latter can be efficiently calculated [11].

Strong disorder.—Results are shown in Fig. 2, where parameters were chosen to obtain a bulk gap $\Delta = 2t$, the hopping strength. System sizes with perimeter $4L$, with $L = 6, 9, 12, 15$ were studied and the quasi-1D localization length λ_φ was extracted as a function of flux. We consider strong disorder, to obtain a localization length short enough to be measured: $W = 2\Delta$ for the first two and $W = 4\Delta$ for the last two sizes. The chemical potential was taken to be near the middle of the gap ($E = 0$), where the Dirac node appears in the clean limit. However, for these strong disorder strengths, results are nearly *independent* of chemical potential location inside the bulk gap. As seen in Figs. 2(a) and 2(b) a clear maximum in localization length is seen near $\varphi = \pi$. Note, the location of the maximum near $\varphi = \pi$ and the $\varphi \to 2\pi - \varphi$ is consistent with time reversal being an approximate symmetry even for the smallest sizes. However at $\varphi = \pi$, the localization length is finite, so time reversal symmetry breaking enters here. Clearly, for larger widths the symmetry is more accurate, given the weaker fields prevailing on the surface states. With the definition $g_\varphi = \lambda_\varphi/4L$, this quantity ranges from $g_0 = 1.6$ to $g_\pi = 6.3$, as the flux is varied, for $L = 15$. Hence, for these parameters, wires with aspect ratios roughly in this range should exhibit conductance oscillations with a maximum at flux π, as shown below.

Weak disorder.—In Fig. 2(d), we plot a system with weak disorder, where $W = 0.5\Delta$, and the chemical potential is tuned to $E = 0.15\Delta$, where there is a large density of states. The localization lengths are now significantly longer

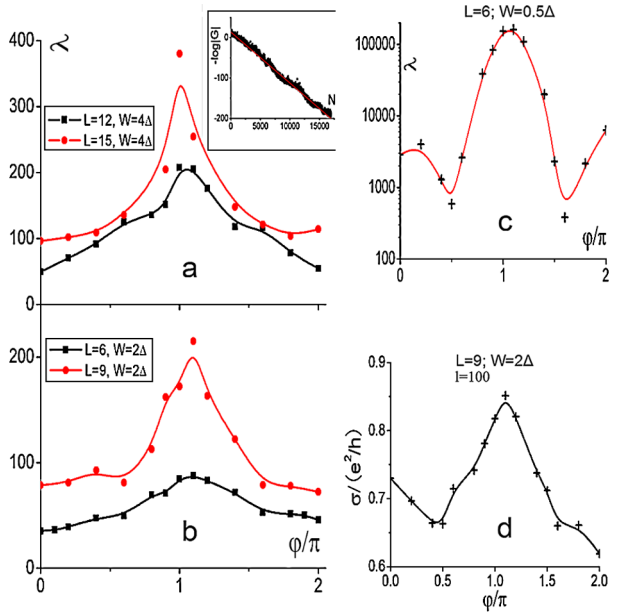

FIG. 2 (color online). (a),(b),(c) Localization length λ in the quasi-1D geometry, for different widths L and disorder strengths W (in units of the bulk gap Δ). Error bars are smaller than the symbol size. (a) and (b) Strong disorder: variation has flux-period hc/e and λ is maximum at flux $\varphi = \pi$. Inset: Example of the exponential decay of the Green's function used to determine λ. (c) Weak disorder: the $hc/2e$ oscillation period is also apparent and localization lengths are large (note log scale here). (d) Conductance oscillation: measure of conductance for a wire of length $l = 100$ and width $L = 9$, with strong disorder $W = 2\Delta$. Maximum conductance occurs at π flux.

(note the log scale for λ), and a prominent antilocalization feature is present near flux $\varphi = \pi/2, 3\pi/2$. The latter will contribute to an AAS $hc/2e$ period in conductance oscillations. Since $g_0 = 125$, at smaller aspect ratios the system is unaware that there is an even longer localization length at π flux, and the most visible feature is likely to be the $hc/2e$ AAS oscillations. This illustrates the important role of strong disorder in observing the effect of interest.

Conductance.—Finally, in Fig. 2(d), we present the conductance of a wire with length $l = 100$, cross section 9×9, and strong disorder strength $W = 2\Delta$. The conductance is extracted from the Greens function using the Kubo formula, $\sigma = \frac{e^2\hbar}{\pi l^2} \mathrm{Tr}[v_z \mathrm{Im}\mathbf{G} v_z \mathrm{Im}\mathbf{G}]$ with $v_z = \frac{i}{\hbar}[H, z]$. The effect of leads is modeled by sandwiching the disordered system between 4×10^3 layers of clean wire on either side. We take $\mu = 0.15\Delta$, to obtain a finite density of states in the leads. The localization length for these parameters is close to that in Fig. 2(b), so l is intermediate between the localization lengths obtained there. A small imaginary part $\epsilon \sim 5 \times 10^{-4}\Delta$ is inserted in the energy to obtain finite results; results are insensitive to its precise value. Each data point is obtained by averaging log of conductance over 500 samples. Clearly, a conductance maximum at flux π is observed. Note, however, the $hc/2e$ oscillations are more prominent here than in

the localization length plots, and the overall contrast in conductance is of order $0.1e^2/h$. This will increase for longer wires and wider cross sections, where the effects of $\mathcal{T}$ breaking at π flux are less important, and localization of states away from this flux will set in. While a more extensive conductance analysis is left to the future, these results corroborate the basic picture.

Scaling analysis.—How do these results scale to larger system sizes, as in the experiments [10]? We examine this first at zero and then at π flux. (i) In the truly two-dimensional limit a metallic (symplectic metal) phase is expected, hence $g_0(L \to \infty) \to \infty$, this growth is slow. The scaling to larger widths is captured by the beta function $\beta(g) = d\log g/d\log L$, similar to the well known beta function for conductance. This function is known for spin-orbit metals in 2D [14]. For large g, the topological insulator surface displays identical behavior [15]; i.e., $\beta(g) \sim 0.64/g$. We estimate this to be reasonably accurate for $g \geq 2$ for TI surfaces; integrating which yields: $\lambda_0(\tau L) \approx \lambda_0(L) + 2.56L\log\tau$. (ii) The localization length at π flux diverges more rapidly, since the effects of $\mathcal{T}$ breaking are weaker at larger widths. It is readily seen that this scales asymptotically as $\lambda_\pi(L) \sim L^4$ (since $\mathcal{T}$ breaking strength scales as $\delta \sim 1/L^2$, and the localization length for weak δ scales as $\lambda \sim 1/\delta^2$). Thus the ratio $\lambda_\pi/\lambda_0 \sim L^3/\log L$ diverges with increasing cross section, implying a wide range of intermediate wire lengths $\lambda_0 \ll l_z \ll \lambda_\pi$ where the zero flux state appears localized, but the π flux state is extended.

Experimental realization.—In Ref. [10], Bi_2Se_3 nanowires with circumference 350 nm and length 2 μm were studied. We simulated models roughly 10 times narrower in width. An important question we address is the effect of finite $\mathcal{T}$ breaking induced by the field. This ultimately leads to localization even at π flux. However, our numerical experiments already demonstrate very long localization lengths at this flux, while the zero flux state is well localized. The larger experimental cross sections will further enhance this contrast, as discussed above. We checked that the *Zeeman* splitting induced by the field in the numerical simulations does not affect results qualitatively, if their energy scale $E_z \leq 0.025\Delta$. This should be readily satisfied in experiments. Note, we have ignored electron interactions, which is an interesting subject for future research. However, given the large dielectric constants of these materials (e.g., $\epsilon \sim 100$ in Bi_2Te_3, [16]), this is a reasonable first approximation. For the disorder strengths assumed here, wires with the experimental dimensions would clearly exhibit the anomalous AB effect. Thus, the main requirement for a given length of nanowire appears to be strong disorder, so one is in the localized regime at zero flux. We believe this is not met in the present experiments [10], but could be achieved via greater surface disorder, or tuning the chemical potential to an energy with smaller carrier density.

Conclusions.—We described a topological property of the surface states of TIs. An Aharonov-Bohm phase of π strengthens the metallic nature of surface states, leading to a clear-cut transport signature. Our work is summarized in Fig. 2(d), the result of a numerical experiment on a "nanowire" of TI, which shows a conductivity maximum at π flux. The conductance is slightly smaller than the ideal e^2/h value due to weak $\mathcal{T}$ breaking. The key requirements for observing this effect are quasi-one-dimensionality and strong disorder, which we believe are achievable given current experimental capabilities.

We acknowledge insightful discussions with H. Mathur, D. Carpentier, J. Moore, and G. Paulin, and DOE Grant No. DE-AC02-05CH11231 for support. In [17], broadly similar results are obtained using a 2D Dirac treatment, although, in contrast to our 3D model calculation, surface curvature Berry phase and finite $\mathcal{T}$ breaking at π flux are not included in that approximation.

[1] M. Z. Hasan and C. L. Kane, arXiv:1002.3895v1 [Rev. Mod. Phys. (to be published)]; X.-L. Qi and S.-C. Zhang, Phys. Today **63**, No. 1, 33 (2010); J. E. Moore, Nature (London) **464**, 194 (2010).
[2] T. Eguchi, P. Gilkey, and A. Hansen, Phys. Rep. **66**, 213 (1980).
[3] Y. Zhang, Y. Ran, and A. Vishwanath, Phys. Rev. B **79**, 245331 (2009).
[4] P. M. Ostrovsky, I. V. Gornyi, and A. D. Mirlin, Phys. Rev. Lett. **105**, 036803 (2010); G. Rosenberg, H.-M. Guo, and M. Franz, Phys. Rev. B **82**, 041104 (2010).
[5] C. L. Kane and E. J. Mele, Phys. Rev. Lett. **95**, 226801 (2005).
[6] R. A. Webb *et al.*, Phys. Rev. Lett. **54**, 2696 (1985); V. Chandrasekhar *et al.*, Phys. Rev. Lett. **55**, 1610 (1985).
[7] A. D. Stone and Y. Imry, Phys. Rev. Lett. **56**, 189 (1986).
[8] B. L. Altshuler, A. G. Aronov, and B. Z. Spivak, Pis'ma Zh. Eksp. Teor. Fiz. **33**, 101 (1981) [JETP Lett. **33**, 94 (1981)]; D. Y. Sharvin and Y. V. Sharvin, Pis'ma Zh. Eksp. Teor. Fiz. **34**, 285 (1981) [JETP Lett. **34**, 272 (1981)].
[9] V. L. Nguyen, B. Z.Spivak, and B. I. Shklovskii, Pis'ma Zh. Eksp. Teor. Fiz. **41**, 35 (1985) [JETP Lett. **41**, 42 (1985)].Y. Avishai and R. Horowitz, Phys. Rev. B **35**, 423 (1987).
[10] H. Peng *et al.*, Nature Mater. **9**, 225 (2010).
[11] See supplementary material at http://link.aps.org/supplemental/10.1103/PhysRevLett.105.206601 for Dirac theory on a curved surface.
[12] Y. Ran, Y. Zhang, and A. Vishwanath, Nature Phys. **5**, 298 (2009).
[13] L. Fu, C. L. Kane, and E. J. Mele, Phys. Rev. Lett. **98**, 106803 (2007).
[14] Y. Asada, K. Slevin, and T. Ohtsuki, Phys. Rev. B **70**, 035115 (2004).
[15] K. Nomura, M. Koshino, and S. Ryu, Phys. Rev. Lett. **99**, 146806 (2007); J. H. Bardarson *et al.*, Phys. Rev. Lett. **99**, 106801 (2007).
[16] D. L. Greenaway and G. Harbere, J. Phys. Chem. Solids **26**, 1585 (1965).
[17] J. Bardarson, P. Brouwer, and J. Moore, Phys. Rev. Lett. **105**, 156803 (2010).